

Coherent locator approach to lattice vibrations in alloys with diagonal and geometrically-scaled off-diagonal disorder

Mark Mostoller and Theodore Kaplan

Solid State Division, Oak Ridge National Laboratory, Oak Ridge, Tennessee 37830

(Received 5 October 1978)

A single-site coherent locator approach to lattice vibrations in alloys with both mass disorder and force-constant changes which obey geometric scaling has been proposed by Grünwald. We show that this theory reduces to a virtual-crystal form for the special case of "equal" mass and force-constant changes, and that it fails to give satisfactory spectral limits for one- and three-dimensional model alloys.

I. INTRODUCTION

Some years ago, a major advance in the theory of alloys was made with the introduction of the coherent potential approximation (CPA). As originally presented by Taylor¹ for phonons and by Soven² for electrons, the CPA was a single-site mean-field theory for diagonal disorder only, that is, for mass changes for lattice vibrations and for random site-diagonal energies for electrons. Changes in the interatomic force constants or transfer integrals were not included in the CPA.

Subsequent to this early work, a number of methods were proposed to include off-diagonal disorder within the framework of a single-site CPA approach. For lattice vibrations, the present authors³ extended the CPA to include force-constant changes as well as mass disorder for alloys in which the force constants superimpose linearly. In simple binary alloys of the form $A_{1-c}B_c$, the assumption of linear superposition is the so-called additive limit, in which the AB force constants are the arithmetic average of the AA and BB force constants, $\Phi_{AB} = \frac{1}{2}(\Phi_{AA} + \Phi_{BB})$.

Somewhat more work has been done to include off-diagonal disorder for electrons in alloys. Fukuyama *et al.*⁴ presented the electronic version of the CPA in the additive limit after the corresponding treatment for phonons had appeared. Earlier, Shiba⁵ described a single-site coherent locator approach for the case in which the interatomic transfer or hopping integrals scale geometrically, $\Phi_{AB} = (\Phi_{AA}\Phi_{BB})^{1/2}$. Blackman, Esterling, and Berk⁶ generalized the coherent locator treatment to include arbitrary changes in the transfer integrals. Perhaps the most general single-site theory for electrons in alloys is the muffin-tin CPA of Soven⁷; this has only recently been implemented by Stocks and co-workers,⁸ and there is no obvious analog for phonons.

Except in the additive limit,⁹ it has not been clear that the coherent locator approach can be

applied to lattice vibrations. As will be discussed directly, the reason for this is that translational invariance imposes an additional formal constraint for phonons that is not required for electrons. Grünwald¹⁰ has recently proposed a coherent locator treatment for lattice vibrations in the geometric limit, i.e., for the case in which the off-diagonal force-constant matrices scale geometrically. In Sec. II, we review the basic features of Grünwald's theory, and describe how it reduces to analytically soluble equations for the special case of "equal" mass and force-constant changes and for disordered linear chains. Section III is devoted to comparisons between essentially exact results for linear chains and those obtained by using the coherent locator approach. Conclusions and some results for three dimensions are discussed in Sec. IV.

II. THEORETICAL MODEL

The problem encountered in attempting to extend a single-site coherent locator approach to phonons in alloys is that translational invariance must be obeyed. Let $\underline{\Phi}(l, l')$ be the force-constant matrix connecting sites l and l' in the alloy. Then in order that no vibrations be excited in a uniform translation of the crystal, the force constants must satisfy the sum rules

$$\underline{\Phi}(l, l) = - \sum_{l' \neq l} \underline{\Phi}(l, l'). \quad (1)$$

If there is disorder in the off-diagonal (interatomic) force constants, then this is necessarily reflected by changes in the diagonal (intra-atomic) terms in the Hamiltonian. No such formal constraint is operative for electrons. In the additive limit for phonons, Eq. (1) is satisfied automatically by appropriately defined perturbations associated with single sites.³ In general, however, and in the geometric limit, it is not possible to represent the force-constant changes in the alloy as

a sum of perturbations associated with single sites.

In Grünewald's coherent locator approximation for the geometric limit, which we will call the CPA-G, all of the correlations between off-diagonal and diagonal disorder which follow from Eq. (1) are not included. Instead, Eq. (1) is used to derive two sum rules for the configurationally averaged Green's functions in the alloy. Imposing these as additional constraints on the coherent locator development leads to a closed set of equations from which the site-diagonal, CPA-G self-energy can be calculated. We will give a very brief outline of the approach in the next few paragraphs.

The time transform of the displacement-displacement Green's function, denoted by $\underline{G}(l, l'; \omega)$, satisfies the equation

$$\delta(l, l') \underline{I} = \sum_{l_1} [M(l) \omega^2 \delta(l, l_1) \underline{I} - \underline{\Phi}(l, l_1)] \cdot \underline{G}(l_1, l'; \omega), \quad (2)$$

where $M(l)$ is the mass of the atom at site l , ω is the frequency, and \underline{I} is the unit matrix. Let $A(l)$ be any quantity which depends on the type of atom which occupies site l , and N be the number of atoms in the crystal. If we multiply Eq. (2) by $A(l')/N$, sum over l and l' , use Eq. (1), and take the configurational average, we obtain

$$\langle A(l) \rangle \underline{I} = \omega^2 \left(\frac{1}{N} \sum_{l, l'} \langle M(l) \underline{G}(l, l'; \omega) A(l') \rangle \right). \quad (3)$$

Grünewald's Eqs. (2.16) and (2.17) are equivalent to Eq. (3) for the choices $A(l) = 1$ and $A(l) = M(l)$.

With geometric scaling, the interatomic force constants can be written in the form

$$\underline{\Phi}(l, l') = \lambda(l) \underline{\Phi}^{\text{eff}}(l, l') \lambda(l'), \quad l \neq l', \quad (4)$$

where $\lambda(l) = 1$ if there is a host atom at the site l , and $\lambda(l) = \lambda$ for a defect atom at l . Grünewald's coherent locator expansions for the four Green's functions \underline{G} , \underline{H} , $\underline{\tilde{H}}$, and \underline{F}' (displacement-displacement, displacement-momentum, momentum-displacement, momentum-momentum) can be reduced to an expansion for a single Green's function defined by

$$\underline{g}(l, l'; \omega) = \lambda(l) \underline{G}(l, l'; \omega) \lambda(l'). \quad (5)$$

A mean-field CPA-like Green's function $\tilde{\underline{G}}(l, l; \omega)$ is then constructed by requiring that $\langle \underline{g}(l, l') \rangle = \tilde{\underline{G}}(l, l')$ for $l = l'$, and that Eq. (3) be satisfied for two choices of $A(l)$:

$$\tilde{\underline{G}}(0, 0; \omega) = \langle \underline{g}(l, l; \omega) \rangle, \quad (6)$$

$$\begin{aligned} & \langle A_i(l) \rangle \underline{I} \\ &= \omega^2 \left(\frac{1}{N} \sum_{l, l'} \left\langle \frac{M(l)}{\lambda(l)} \underline{g}(l, l'; \omega) \frac{A_i(l')}{\lambda(l')} \right\rangle \right), \quad i = 1, 2. \end{aligned} \quad (7)$$

As already noted, Grünewald's two choices for $A_i(l)$ are $A_1(l) = 1$ and $A_2(l) = M(l)$, but in fact any two (different) functions $A_i(l)$ of the site-occupation variables yield the same results.

For cubic crystals, the effective-medium Green's function $\tilde{\underline{G}}$ is defined in terms of a site-diagonal, scalar self-energy $\tilde{\epsilon}(\omega)$ and the host force constants $\underline{\Phi}^{\text{eff}}(l, l')$ by

$$\begin{aligned} \delta(l, l') \underline{I} = & \sum_{l_1} \{ M \omega^2 [1 - \tilde{\epsilon}(\omega)] \delta(l, l_1) \underline{I} \\ & - \underline{\Phi}^{\text{eff}}(l, l_1) \} \cdot \tilde{\underline{G}}(l_1, l'; \omega), \end{aligned} \quad (8)$$

where M is the host mass. The self-energy in turn satisfies the self-consistent equation

$$\begin{aligned} 0 = & \tilde{\epsilon}(\omega) + \frac{c\Delta}{1-c\Delta} + \frac{c(\Delta-\epsilon)}{(1-c\Delta)^2} \\ & + \left(\tilde{\epsilon}(\omega) + \frac{c\Delta}{1-c\Delta} \right) \left(\tilde{\epsilon}(\omega) + \frac{\beta+c\Delta}{1-c\Delta} \right) \omega^2 f(\omega). \end{aligned} \quad (9)$$

Here $\epsilon = 1 - M_d/M$, $\Delta = 1 - \lambda$, and $\beta = (1 - \epsilon)/\lambda - 1$. The concentration of defects is c , and $f(\omega) = M \tilde{\underline{G}}_{\alpha\alpha}(0, 0; \omega)$.

Consider now the special case of "equal" changes in the masses and force constants, that is,

$$\epsilon = \Delta; \quad M_d/M = \lambda. \quad (10)$$

For this case $\beta = 0$, and Eq. (9) reduces to

$$\begin{aligned} 0 = & [\tilde{\epsilon}(\omega) + c\epsilon/(1-c\epsilon)] \\ & \times \{ 1 + [\tilde{\epsilon}(\omega) + c\epsilon/(1-c\epsilon)] \omega^2 f(\omega) \}. \end{aligned} \quad (11)$$

By retracing the derivation of Eq. (9) for $\epsilon = \Delta$, it can be established that the proper root to choose from Eq. (11) is

$$\tilde{\epsilon}(\omega) = -c\epsilon/(1-c\epsilon), \quad (12)$$

which is simply a constant independent of ω . This surprising result, which is true for one, two, and three dimensions, can be confirmed analytically for one-dimensional alloys. In one dimension, as will be discussed shortly, Eq. (9) becomes a cubic equation for $\tilde{\epsilon}(\omega)$. For $\epsilon = \Delta$, the expression in Eq. (12) is a double root of this cubic equation, and the third root, which is also real, gives a vanishing alloy density of states for all ω .

Corresponding to the real self-energy in Eq. (12), the density of states for the alloy for $\epsilon = \Delta$ is found to be

$$\langle \nu(\omega) \rangle = \frac{1}{\sqrt{1-c\epsilon}} \nu_{\text{eff}} \left(\frac{\omega}{\sqrt{1-c\epsilon}} \right), \quad (13)$$

where $\nu_{\text{eff}}(\omega)$ is the density of states for the perfect host crystal of atoms of mass M coupled by force constants $\Phi^{\text{eff}}(l, l')$. Equations (12) and (13) have the same form as virtual-crystal results: the self-energy is real, and the alloy appears like a perfect crystal with (real) masses or force constants modified from their values in the host. Phonons in the alloy for the special case $\epsilon = \Delta$ are not broadened, but have infinite lifetimes. The alloy density of states given in Eq. (13) is that for a perfect crystal comprised of atoms of mass $M' = M/(1 - c\epsilon)$ and force constants $\Phi^{\text{eff}}(l, l')$. If ω_0 is the maximum host-crystal frequency, then $\omega'_0 = \omega_0\sqrt{1 - c\epsilon}$ is the maximum frequency predicted for the alloy. We emphasize that Eqs. (12) and (13) are general results for the special case $\epsilon = \Delta$, and are not restricted to one-dimensional alloys.

For one-dimensional alloys with first-nearest-neighbor interactions, the function $f(\omega)$ $= M\bar{G}(0, 0; \omega)$ can be evaluated analytically,

$$\omega^2 f(\omega) = (\omega/\omega_0) \{ [1 - \bar{\epsilon}(\omega)] \{ (\omega/\omega_0)^2 [1 - \bar{\epsilon}(\omega)] - 1 \} \}^{-1/2}, \quad (14)$$

where $\omega_0 = [-4\Phi^{\text{eff}}(l, l+1)/M]^{1/2}$ is the maximum host-crystal frequency. Substituting this into Eq. (9), we obtain a cubic equation for the self-energy. Once the proper root of this cubic equation for $\bar{\epsilon}(\omega)$ is chosen, the CPA-G density of states can be found directly, and compared with the results of exact calculations.

III. RESULTS FOR ONE-DIMENSIONAL ALLOYS

In this section, we will quickly run through a number of examples for disordered linear chains, comparing the densities of states predicted by Grünewald's coherent locator approach with essentially exact results obtained by node counting¹¹ for chains of 10 000 atoms. To provide additional perspective, a few examples of mass-defect and additive-limit CPA calculations will also be discussed.

Figure 1 compares CPA-G and exact results for the special case of "equal" mass and force-constant changes, $\epsilon = \Delta = 1 - \lambda$. The results shown are for lighter mass impurities with reduced force constants at a defect concentration of $c = 0.4$. The CPA-G density of states compares poorly with the exact results: it is a virtual-crystal-like curve in which the only effect of alloying is a change of bandwidth to a value roughly 20% too low. Quite similar results are obtained for heavier mass impurities with increased forces for the special case $\epsilon = \Delta$.

Figure 2 compares CPA-G and exact results for force-constant changes only ($\epsilon = 0$) at a defect con-

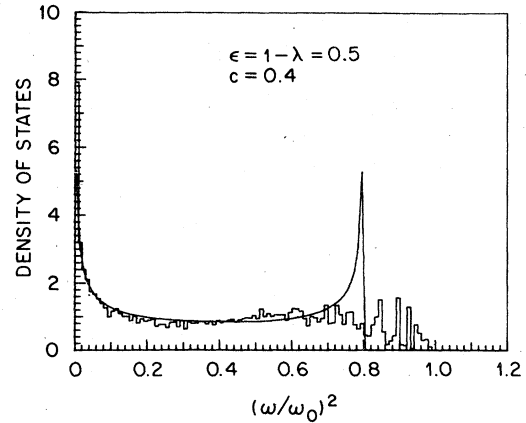


FIG. 1. CPA-G (smooth curve) and exact results (histogram) for equal mass and force-constant changes, $\epsilon = \Delta = 1 - \lambda$. In these and all succeeding figures save Fig. 7, results are plotted vs $(\omega/\omega_0)^2$, where ω_0 is the maximum frequency in the host crystal. All densities of states shown are normalized to integrate to unity.

centration of $c = 0.2$ for increased force constants. In this example, the CPA-G again yields a spectrum appreciably narrower than the exact results. In addition, the CPA-G curve has a peak where the exact calculations show a valley between the host-crystal band edge and the first impurity peak.

As discussed in Sec. I, the two special cases of off-diagonal disorder for which extensions of the CPA have been proposed for lattice vibrations are the additive and geometric limits. We have been using CPA-G to denote Grünewald's coherent locator approach for force constants which scale geometrically; the single-site CPA developed by the present authors³ to include additive force-con-

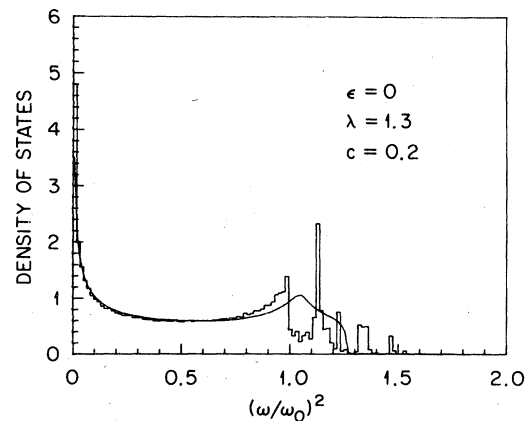


FIG. 2. CPA-G and exact results for force-constant changes only.

stant changes will be referred to as the CPA-F. Figure 3 gives illustrative CPA-F results for comparison with the CPA-G results in Fig. 2. For the example shown in Fig. 3, there are no mass changes, the concentration is the same as in Fig. 2, and the force constants in the additive limit are chosen to give the same pure-material bandwidth as the geometrically scaled force constants in Fig. 2:

$$\Phi_{dd} = \lambda^2 \Phi_{hh} = \lambda^2 \Phi^{\text{eff}}; \quad \Phi_{dh} = \Phi_{hd} = \frac{1}{2}(\lambda^2 + 1)\Phi_{hh}.$$

Although it underestimates the maximum frequencies by small amounts, the CPA-F clearly fits the observed bandwidth for the additive limit better than the CPA-G for the geometric limit. Furthermore, the peak in the CPA-F curve coincides with the host-crystal band-edge peak in the exact results.

In Figs. 1 and 2, we have shown two cases for which the CPA-G underestimates the alloy bandwidths. Figures 4 and 5 demonstrate that the CPA-G can also predict broader spectra than actually occur. Figure 4 is for light mass defects with reduced force constants at a defect concentration of $c=0.2$. For this case, the CPA-G density of states not only extends to frequencies which are substantially too high, but also exhibits a peak where none is observed in the exact results. Figure 5 is for heavy impurities with increased force constants at a concentration of $c=0.5$; here, the CPA-G curve is featureless, and cuts off roughly 10% above the histogram of the exact results.

We have performed mass-defect CPA and exact calculations for a single-band case like that in Fig. 5, using the parameters $c=0.5$ as in Fig. 5, $\lambda=1$ (no force-constant changes), and $\epsilon=-0.183$ to give the same pure-material bandwidths for the

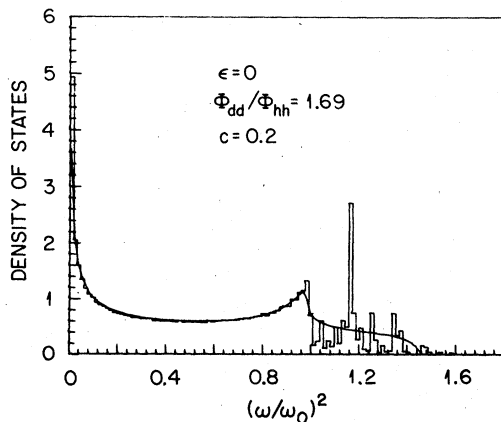


FIG. 3. CPA-F (additive-limit CPA) and exact results for force-constant changes only in the additive limit, $\Phi_{dh} = \Phi_{hd} = \frac{1}{2}(\Phi_{dd} + \Phi_{hh})$.

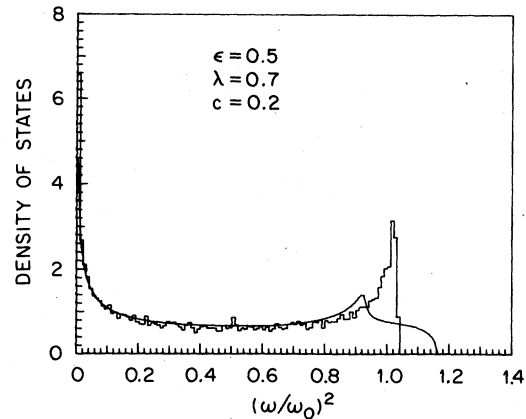


FIG. 4. CPA-G and exact results for light-mass defects with reduced forces.

two constituents (1 and 0.845) as in Fig. 5. The mass-defect CPA yields a curve that runs smoothly through the histogram of the exact results, with the correct bandwidth and no spurious structure.

Figure 6 compares CPA-G and exact results for a case for which local modes above the host-crystal spectrum are introduced by the impurities. The CPA-G fits the exact results reasonably well in the frequency range of the host crystal, and produces a broad, smooth impurity band typical of the mean-field approach, but which ends just below the last sizable peak in the exact results. For comparison, we have also performed CPA and exact calculations for an alloy with mass disorder only, but with the same pure-material bandwidths for the two constituents (1 and 3.38) as in Fig. 6. We found that the impurity band in the mass-defect CPA spans the peak missed by the CPA-G in Fig. 6, and the agreement between the

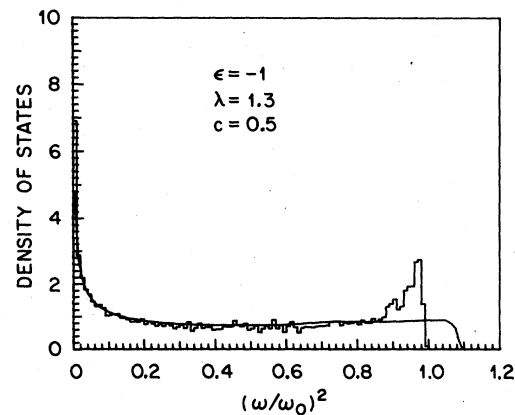


FIG. 5. CPA-G and exact results for heavy impurities with increased force constants.

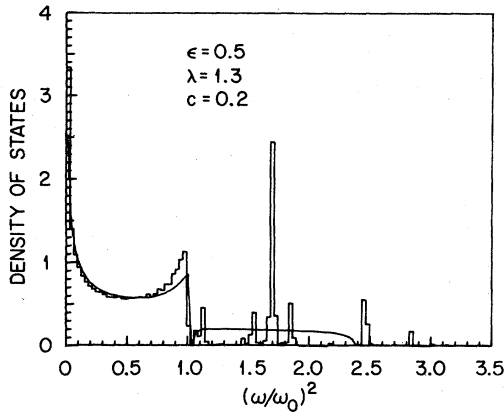


FIG. 6. CPA-G and exact results for light-mass defects and increased force constants.

CPA and exact results in the host-crystal frequency range is somewhat better.

IV. CONCLUSIONS

The single-site coherent locator approach proposed by Grünewald for alloys with both mass disorder and force-constant changes which scale geometrically has a number of limitations. Like other single-site CPA theories, it can at best give only an approximate, overall picture of alloy properties, and cannot reproduce structure in spectral functions arising from pair and larger cluster correlations. However, unlike the CPA for mass defects or the CPA-F which includes force-constant changes in the additive limit, the CPA-G reduces to a virtual-crystal form for certain sets of parameters (corresponding to "equal" mass and force-constant changes) at all concentrations in one, two, or three dimensions. From the results for disordered linear chains shown in Sec. III, it appears that the CPA-G also does a relatively poor job of predicting alloy bandwidths, underestimating noticeably in some instances, overestimating in others.

There is another limiting feature of the CPA-G treatment that we have not previously drawn attention to, but which should be emphasized. Because the CPA-G self-energy is site diagonal, it depends only on the phonon frequency ω and not on the wave vector \vec{q} ; as such, it cannot be expected to lead to the wave-vector or phonon branch dependence observed in the coherent neutron scattering from some alloys.¹²

The CPA-G has been applied to phonons in K_cRb_{1-c} alloys.¹³ This is perhaps the most extensively studied system for lattice vibrations in random alloys. Neutron scattering measurements

have been performed by Kamitakahara and Copley¹⁴ at potassium concentrations of $c = 0.06, 0.18,$ and 0.29 . Mass-defect CPA calculations have been done,¹⁴ as have CPA-F calculations including first-nearest-neighbor radial force-constant changes in the additive limit.¹⁵ Molecular dynamics simulations have also been carried out for K_cRb_{1-c} alloys.¹⁶

We will not attempt to give a complete summary of all of these studies, but will briefly touch on a few important points. The experiments found a quite distinct two-peaked structure in the neutron groups at momentum transfers near the zone-boundary wave vectors $\vec{Q} = (2\pi/a)(2.5, 2.5, 0)$ and $\vec{Q} = (2\pi/a)(2, 2, 1)$. This structure was poorly reproduced by mass-defect CPA calculations. When force-constant changes in the additive limit were included in CPA-F calculations performed by the present authors,¹⁵ the agreement with experiment improved, but not to a completely satisfactory level. This led us to suggest that multisite scattering effects were important in the K_cRb_{1-c} alloy system.

The coherent locator or CPA-G results¹³ appear to fit the experimental data somewhat better than the other single-site CPA calculations. For scattering wave vectors $\vec{Q} = (2\pi/a)(2 + \zeta, 2 + \zeta, 0)$ at concentrations of $c = 0.18$ and 0.29 , the CPA-G (geometric limit) and CPA-F (additive limit) calculations give comparable agreement with experiment; the neutron scattering peak positions are fitted reasonably well, but the calculated peaks are not as sharply delineated as those observed. For $\vec{Q} = (2\pi/a)(2, 2, \zeta)$ at $c = 0.29$, the CPA-G scattering cross sections are in better agreement with the data than the CPA-F curves, again giving relatively good values for the peak positions but not reproducing the distinct two-peaked structure observed near the zone boundary. No CPA-G results are given in Ref. 13 for $c = 0.06$ or $\vec{Q} = (2\pi/a)(2, 2, \zeta)$ at $c = 0.18$.

By comparing with exact results for one-dimensional alloys, we have demonstrated that the CPA-G theory for phonons suffers from several general limitations. Figure 7 presents some evidence of the limitations of the CPA-G in three dimensions in general and for K_cRb_{1-c} alloys in particular. For these results, a first- and second-neighbor force model obeying geometric scaling was constructed following the procedure outlined by Grünewald and Scharnberg.¹³ The K-K force constants were taken from Fig. 1 in Ref. 13 at a concentration of $c = 0.29$, and the Rb-K and Rb-Rb forces were then scaled geometrically from the K-K interactions by factors of $\lambda = 1.28$ and λ^2 . This differs from the force model used in Ref. 13 only in the absence here of third- and fourth-neighbor

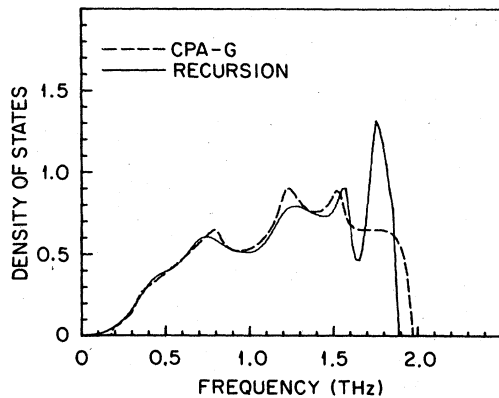


FIG. 7. CPA-G and recursion results for $K_{0.29}Rb_{0.71}$ with mass and force-constant changes corresponding to those in Ref. 13. Note that results here are plotted against $\nu = \omega/2\pi$ (THz).

interactions.

The dashed curve in Fig. 7 is the CPA-G density of states for the model $K_{0.29}Rb_{0.71}$ alloy, while the solid line gives results obtained by the recursion method¹⁷ for 400 clusters of 4641 atoms. For single-band cases, that is, for situations where the spectrum of excitations forms one continuous

band rather than two or more separated by regions of zero spectral density, the recursion method provides an accurate description of the major spectral features, particularly of the band limits.¹⁸ Figure 7 illustrates two of the deficiencies attributed to the CPA-G theory at the outset of this section. First, the CPA-G bandwidth is noticeably too broad. Second, the CPA-G gives only a broad shoulder in the local-mode region, while recursion shows that the local-mode peak at $\nu \sim 1.75$ THz is the most prominent feature of the spectrum. As we have noted previously,¹⁵ the inability to reproduce sharp structure in spectral functions is a characteristic feature of single-site mean-field approaches, which indicates the need to adopt more sophisticated analytical methods or to move toward brute-force calculations to incorporate the cluster-scattering and local-environment effects absent in the single-site theories.

ACKNOWLEDGMENTS

The authors are grateful to N. Wakabayashi for helpful conversations. This research was sponsored by the Division of Materials Sciences, U. S. Department of Energy under contract W-7405-eng-26 with the Union Carbide Corporation.

¹D. W. Taylor, Phys. Rev. **156**, 1017 (1967).

²P. Soven, Phys. Rev. **156**, 809 (1967).

³T. Kaplan and M. Mostoller, Phys. Rev. B **9**, 1783 (1974).

⁴H. Fukuyama, H. Krakauer, and L. Schwartz, Phys. Rev. B **10**, 1173 (1974).

⁵H. Shiba, Prog. Theor. Phys. **46**, 77 (1971).

⁶J. A. Blackman, D. M. Esterling, and N. F. Berk, Phys. Rev. B **4**, 2412 (1971).

⁷P. Soven, Phys. Rev. B **2**, 4715 (1970).

⁸G. M. Stocks, W. M. Temmerman, and B. L. Gyorffy, Phys. Rev. Lett. **41**, 339 (1978).

⁹K. Niizeki, Prog. Theor. Phys. **53**, 74 (1975); **54**, 1648 (1975).

¹⁰G. Grünewald, J. Phys. F **6**, 999 (1976).

¹¹P. Dean, Proc. R. Soc. Lond. A **260**, 263 (1961); Rev. Mod. Phys. **44**, 127 (1972).

¹²See, for example, E. C. Svensson, B. N. Brockhouse, and J. M. Rowe, Solid State Commun. **3**, 245 (1965);

E. C. Svensson and B. N. Brockhouse, Phys. Rev. Lett. **18**, 858 (1967); R. Bruno and D. W. Taylor, Can. J. Phys. **49**, 2496 (1971); K. M. Kesharwani and B. K. Agrawal, Phys. Rev. B **7**, 5153 (1973).

¹³G. Grünewald and K. Scharnberg, in *Proceedings of the International Conference on Lattice Dynamics*, edited by M. Balkanski (Flammarion, Paris, 1978), p. 443.

¹⁴W. A. Kamitakahara, Bull. Am. Phys. Soc. **19**, 321 (1974); W. A. Kamitakahara and J. R. D. Copley, Solid State Division Annual Progress Report, Oak Ridge National Laboratory Report No. ORNL-4952, 1973 (unpublished).

¹⁵M. Mostoller and T. Kaplan, Phys. Rev. B **16**, 2350 (1977).

¹⁶G. Jacucci, M. L. Klein, and R. Taylor, Phys. Rev. B **18**, 3782 (1978).

¹⁷R. Haydock, V. Heine, and M. J. Kelly, J. Phys. C **5**, 2845 (1972); **8**, 2591 (1975).

¹⁸M. Mostoller and T. Kaplan (unpublished).